RSC Advances

ROYAL SOCIETY OF CHEMISTRY

www.rsc.org/advances

Ag dendritic nanostructures for rapid detection of thiram based on surface-enhanced Raman scattering

Qiang Wang, Dun Wu,Zhidong Chen*
Department of Materials Science and Engineering, Changzhou University , Changzhou,Jiangsu, 243106,P.R. China.
. E-mail: wq@cczu.edu.cn Tel:86-519-86330100

Surface-enhanced Raman scattering (SERS) has been proved to be one of powerful analytical tools for the detection of trace molecules owing to its integration of high sensitivity, unique spectroscopic fingerprint, and non-destructive data acquisition. However, the lacking of reliable, stable, well-defined and uniform SERS substrates impedes their further practical applications in various fields. Herein, we have developed a SERS-active substrate based on Ag dendrites for sensitive Raman signal readout and trace detection of pesticide residues in agricultural products and environments. The SERS substrate can be employed to detect rhodamine 6G (R6G) with an enhancement factor (EF) of 3.18×10^8 and the pesticide thiram in commercial grape juice with a detection limit of as low as 0.1μM (0.03 ppm), which is much lower than the maximal residue limit (MRL) of 7 ppm in fruit prescribed by the U.S. Environmental Protection Agency (EPA). Furthermore, spiked detection indicated that the Ag dendritic substrate can be used to monitor thiram in commercial grape juice and natural lake water without further treatment.

1. Introduction

Since it was discovered on a roughened Ag electrode surface 40 years ago, the surface enhanced Raman scattering (SERS) spectroscopy has become one of the most widely pursued spectroscopic tools for the powerful and extremely sensitive analytical technique with applications in chemical production, biochemistry, and environmental monitoring because of its integration of unique spectroscopic fingerprint, high sensitivity, and non-destructive data acquisition.[1] Over the past decades, many methods, including nanoimprint lithography, focus ion beam lithography, colloidal lithography, e-beam lithography, and self-assembly of nanoparticles (NPs), have been applied to fabricate various SERS-active substrates.[2-5] The principal amplification of SERS arises from the enhancement of the local electromagnetic (EM) fields near appropriately nanostructured metal systems generated by excitation of surface plasmon resonances. It is well known that the strong SERS signals achieved are undoubtedly dominated by signals originating from molecules located on nanogaps or clefts where the electromagnetic field is largely enhanced, which are called "hot spots".[6-8] Until now, most of the SERS active substrates focused on noble metal nanoparticles where tremendous Raman enhancement factors could be obtained in areas of "hot spots" at the junction of neighboring nanostructures.[5] However, hot spots in these substrates are randomly distributed and it is very difficult for the targets to enter the conjunctions among the aggregated NPs. Many researches indicated the controllable, stable, reproducible, and uniform substrate plays a vital role for the giant Raman scattering effect, and the lacking of reliable, stable, well-defined, and uniform SERS substrates impedes their further practical applications.[9-11] Therefore, fabricating a reproducible, ultrasensitive and uniform SERS-active substrates is very desirable for widening its applications in ultrasensitive Raman detection.

Herein, we present a convenient, simple, and rational route for the growth of SERS-active Ag dendritic nanostructures, the substrates for the ultrasensitive detection of trace pesticide residues. The Ag dendritic nanostructures were used as the SERS-active substrate to detect rhodamine 6G (R6G) with an enhancement factor (EF) of as high as ~ 3.18×10^8. Moreover, the as fabricated Ag dendritic nanostructures can be employed to enhance the Raman signals of thiram, reveal a detection limit of as low as 0.03 ppm, which is lower than the U.S. Environmental Protection Agency (EPA) prescribed maximal residue limit (MRL) of 7 ppm in fruit. The simple, rapid and ultrasensitive Raman detection strategy using the Ag dendritic nanostructures detection platform as a Raman amplifier shows great practical potential for the on-site environmental monitoring and the ultrasensitive detection of trace harmful chemicals.

2. Experimental section

2.1 Materials

Thiram, rhodamine 6G (R6G), Cu powder(10-40 mesh)，silver nitrate ($AgNO_3$), ethanol were purchased from Sigma. All the chemicals were analytical reagents without further purification. The real lake water was collected from a local lake and the grape juice was bought from supermarket.Ultrapure water (18.2 MΩ) was obtained from a Millipore Milli-Q purification system and used for all solution preparations.

2.2 Fabrication of Ag dendritic nanostructures

The synthesis of Ag dendritic nanostructures was conducted in a conventional three-necked flask. The flask contained 0.07 g Cu powder，0.22 g $AgNO_3$ and 10 ml H_2O at 50 °C without stirring. After reaction for 20 hours, the obtained Ag dendritic nanostructures was followed by washing with ethanol and water three times, respectively.

2.3 Raman detection of R6G in ethanol

10 μL aliquots of Rhodamine 6G (R6G) in ethanol of different concentrations were pipeted onto the Ag dendritic nanostructure SERS substrate and dried in air for SERS detection. The Raman spectra were recorded using 532 nm laser with 1 mW power and 50 × objective (1 μm^2 spot). The integral time is 0.5 s and slit aperture is 50 μm.

2.4 Raman detections of pesticides in ethanol

The ethanol solutions of pesticides were prepared at different concentrations ranging from 1×10^{-4} to 1×10^{-7} M, and the experiments were carried out using the same procedure as described in the above step. 10 μL aliquots of various concentrations of thiram in ethanol were dispersed on the Ag dendritic nanostructure SERS substrate and the Raman spectra were recorded using 532 nm laser with 1 mW power and a 50 × objective (1 μm^2 spot). The integral time was 2 s and the slit aperture was 25 μm.

2.5 Raman detections of pesticides in spiked samples

For the detection of pesticides in spiked samples, 100 μL of the spiked sample solution was diluted in ethanol to 1 mL, then 10 μL of the diluted solution was dispersed on the substrate and the experiments were carried out using the same procedure as described in above steps. The Raman spectra were recorded using 532 nm laser with 1 mW power and a 50 × objective (1 μm^2 spot). The integral time was 2 s and the slit aperture was 25 μm.

2.6 Instrument

The structures of the Ag dendritic samples were characterized by field-emission 100 scanning microscopy (FE-SEM, Sirion 200) and transmission electron microscopy (TEM, JEOL 2010). The crystalline structures and phase of the sample were determined by X-ray powder diffraction (XRD) using an X-ray diffractometer with Cu Kα radiation (λ = 1.5406 Å). Raman measurements were conducted with a Thermo Fisher DXR Raman microscope equipped with a CCD detector with an excitation wavelength of 532 nm. The laser beam was focused to a spot of about 1 μm^2 by a 50 × microscope objective. The Raman spectra were recorded using 532 nm laser with 1 mW power and a 50 × objective (1 μm^2 spot). The integral time was 2 s and the slit aperture was 25 μm.

3. Results and discussion

The Ag dendritic nanostructures were synthesized by a chemical reduced route at mild reaction condition. The obtained Ag samples were first characterized by the field emission scanning electron microscopy (FE-SEM), as shown in Figure 1. Figure 1a is the SEM image of the Ag dendritic nanostrucutres with large scale. The SEM images in Figure 1b and c denmonstrated the detailed morphology of the dendritic nanostrucutres, which consisits of high quanlity branckes. The TEM image (Figure 1d) further confirmed the dendritic shape of the nanostrucutres. The single-crystalline nature of the oriented Ag dendritic structure is confirmed by the corresponding fast-Fourier transformation (FFT) pattern along the constituent nanowire (inserted in Figure S1a). The FFT pattern reveals that the dendritic structure has a cubic crystal structure grown along the [011] direction. The high-resolution TEM image shown in Figure S1b exhibited clear lattice fringes with a d spacing of about 0.24 nm, which agreed well with the d (111) spacing for fcc Ag, confirming that the dendritic structures were well-defined single crystals of silver with [011] as the growth direction. This observation is well matched with the similar silver nanodendrites synthesised in electrochemical method.[12]

For the growth of the dendritic nanostructures, the copper powder was selected as the reducing agent, which might play an important role in the final formation of the dendritic nanostructures. When using other reducing agents, such as citrate sodium and $NaBH_4$, the obtained products only consist of irregular nanoparticles not of the dendritic nanostructures (Seen in Figure S2). The prepared dendritic nanostructures might be formed by a conventional diffusion-limited branching mechanism in our synthesis process. Diffusion-limited branching occurs when the initial growth rate of silver nanocrystal is faster than the diffusion rate of nutrient ions, which results in a depletion zone around the nanocrystal.The subsquent crystal growth are limited by diffusion when such a depletion layer is formed. Since the apexes of a polyhedral crystal protrude further into the region of higher concentration they can grow faster than the central parts of the facets, thus forming branches.[13] For example, $[01\bar{1}]$ direction of silver nanocrystals would initiate fast growth and the subsequent growth along other two crystallographically equivalent directions, $[\bar{1}0\bar{1}]$ and [110],would lead to the formation of symmetric branches on both sides, then repeat it on the main trunks, as proposed by Yang's group in the similar system.[12]

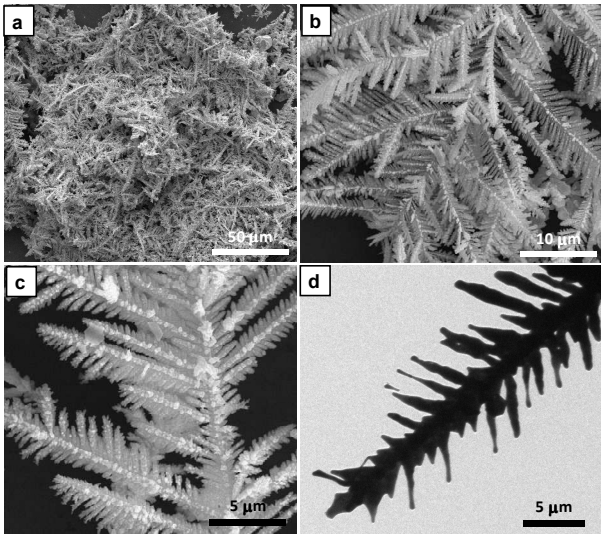

Figure 1. FE-SEM images of the Ag dendritic nanostrucutres: (a) Low magnification and (b) High magnification images of the as-prepared Ag dendritic nanostructures, (c) SEM image of a single dendritic nanostructure; (d) TEM image of a a single dendritic nanostructure.

The resulting Ag dendritic nanostructures are also confirmed by XRD pattern (Figure S3), all of the strong intensity peaks can be indexed to pure face-centered cubic Ag (Joint Committee on Powder Diffraction Standards (JCPDS) card no. 04-0783). The as-obtained Ag dendritic nanostructures can serve as a SERS-active substrate for Raman detection with high sensitivity, good reproducibility and high reliability due to having a large number of hot spots on the surface of the dendritic nanostrucutres. The

junctions of the branches.

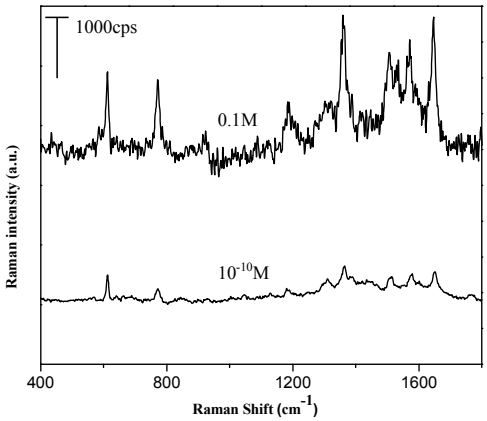

Figure 2. Raman spectra of 0.1 and 1×10^{-10} M rhodamine-6G (R6G) on a silicon substrate (upper) and on the Ag dendrites (bottom), respectively.

Rhodamine (R6G), one of the widely used standard probes for the evaluation of SERS performance, was chosen to probe the SERS effect of the Ag dendritic nanostructured substrate. Figure S4 shows the SERS spectrum obtained by adding 10 μL of R6G in ethanol solution with a concentration ranging from 10^{-8} M to 10^{-10} M by using the Ag dendrites as the substrates. The strong Raman peaks at 612 cm^{-1}, 774 cm^{-1}, 1360 cm^{-1}, 1509 cm^{-1}, and 1650 cm^{-1} are in good agreement with previous reports on pure R6G.[14] The Raman signals can still be observed even when its concentration decreased to as low as 0.1 nM (see Figure 2). Especially，The SERS enhancement factors (EF) for R6G on the Ag dendritic structure can be calculated according to the equation

$$EF= (I_{SERS}/I_{bulk}) (N_{bulk}/N_{surface}),$$

Where I_{SERS} and I_{bulk} are the peak intensities of 0.1 nM R6G on the Ag dendritic nanostructures and 0.1M R6G on a silicon substrate at 612 cm^{-1}, respectively.[15] N_{SERS} and N_{bulk} are the number of R6G molecules excited by the laser beam on the Ag dendritic nanostructures and silicon substrate, respectively. The calculated EF of the Ag dendritic nanostructures is about 3.18×10^8.Furthermore, the SERS spectra of R6G with the concentration of 1×10^{-10} M at random 15 sites on the substrate shows good reproducibility in signal intensity as shown in Figure S5.[16] The experimental results indicated that the Ag dendritic structures has high sensitivity, good flexibility, reproducibility and reliability as the substrate for Raman applications.

Dithiocarbamates are a cluster of organosulfur compounds widely used in industry and agriculture. Thiram (Tetramethylthiuram disulfide) is a dithiocarbamate fungicide, is one of the most widely used in animal repellent and agriculture as a fungicide.[17-18] Moreover, the thiram can lead to serious skin and eye illness, as well as the carbon disulfide release from thiram damage to the liver.[19] Many methods, such as spectrophotometry, colorimetry, chromatography polarography, electrochemical and other have been used to detection thiram.[20-24] However, these techniques are high-cost, complicated and time consuming. To develop simple, rapid, ultrasensitive analytical techniques for the on-site analysis of trace pesticide residues is very urgent. The SERS tool based on the Ag dendritic nanostructure shows potential as a supplemental method for the rapid and sensitive detection of dithiocarbamate chemicals.

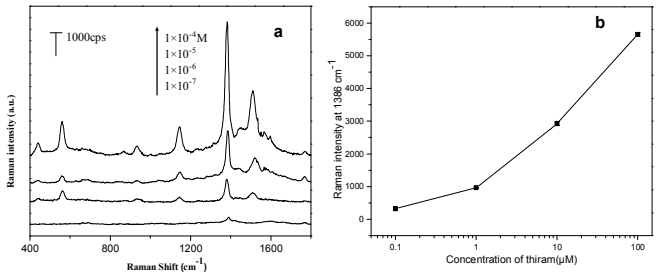

Figure 3. (a) SERS spectra of thiram in ethanol of various concentrations on Ag dendrites; (b) The intensities of SERS signals at 1386 cm^{-1} as the function of the concentrations of thiram in ethanol.

The Ag dendritic nanostructures were further applied for the detection of trace chemicals harmful to the environment. Figure 3a shows the SERS Raman spectra of thiram in ethanol with the concentrations increment from 1.0×10^{-7} to 1.0×10^{-4} M using the Ag dendritic nanostructures as the substrate. The intensity of Raman peaks of thiram located at 560 cm^{-1}, 1148 cm^{-1}, 1386 cm^{-1}, 1507 cm^{-1} increase with the thiram concentration. Figure 4b reflects the relationship between SERS intensity at 1386 cm^{-1} and the concentrations of the thiram in ethanol.

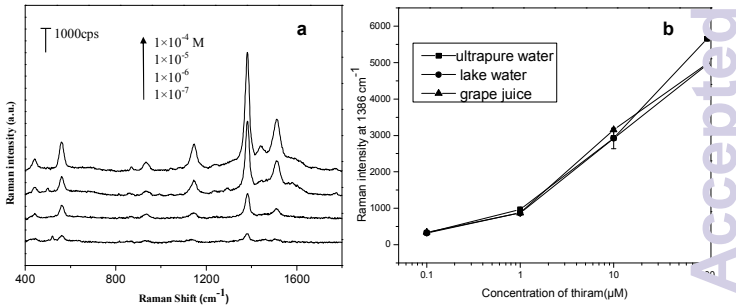

Figure 4. (a) SERS spectra of thiram in grape juice at different spiked concentrations on Ag dendrites; (b) The intensities of SERS signals at 1386 cm^{-1} as a function of the concentrations of thiram spiked in different matrices of natural lake water, grape juice and ultrapure water.

The high Raman sensitivity of the Ag dendritic nanostructures is particularly suitable for the practical monitoring the residual pesticide molecules in various environments. We present the unusual but important applications of the Ag dendritic nanostructures to the identification and detection of thiram residues, in which the other techniques are either undetectable or need complicated sample pretreatments. The spike tests were applied to different matrices, including real lake water, grape juice and ultrapure water. The thiram solution with different concentrations was spiked into real lake water, grape juice and ultrapure water. For the SERS experiment, in order to disperse the sample solution homogeneously on the Ag dendritic nanostructure substrate, 100 μL of the spiked sample solution was diluted in ethanol to 1 mL, and then 10 μL of the diluted solution was pipeted onto the substrate. Figure 4a is the Raman spectra of thiram in grape juice at different spiked concentrations increment from 1.0×10^{-7} to 1.0×10^{-4} M on the Ag dendritic nanostructures, and the Raman intensities of thiram molecules at 1386 cm^{-1} increase with the thiram residue amount in the juice. Significantly, the detection limit of thiram in the grape juice is

1.0×10^{-7} M, which is the same as the detection limit in ethanol. Similar results were obtained by a systematic study on the Raman response to thiram in ultrapure water and real lake water in the same conditions (see Figure S6,S7 in the Supporting Information). Figure 4b reflects the relationship between SERS intensity at 1386 cm^{-1} and the concentrations of the thiram in real lake water, ultrapure water and grape juice. All the fingerprint SERS signals of thiram could be observed clearly from the three samples. The results imply that the as-fabricated Ag dendritic nanostructures can be used to detect thiram in all of the different matrices tested with high sensitivity and good reproducibility. Even at 0.1 μM (0.03 ppm) level, signals of thiram can still be clearly noticed. The detection limit of thiram is lower than the maximal residue limit of 7 ppm in fruit prescribed by the U.S. Environmental Protection Agency (EPA).

4. Conclusion

In summary, we have developed a simple and facile approach for the preparation of the Ag dendritic nanostructures, which can serve as an effective SERS detection platform for environmental monitoring and ultrasensitive detection of the harmful chemicals. Significantly, the Ag dendritic nanostructures exhibits good sensitive Raman signal readout with the SERS enhancement factor of about 3.18×10^{8}. The SERS substrate could produce highly enhanced Raman signals with good uniformity and reproducibility due to tremendous hot spots generated from the unique dendritic structures, which can be applied to monitor the trace chemicals harmful to the environment with ultralow concentrations in environments including thiram. The Ag dendritic substrate can be applied to detect the pesticide thiram in commercial grape juice with a detection limit of as low as 0.1 μM (0.03 ppm), which are several orders of magnitude lower than the maximal residue limit (MRL) in fruit prescribed by U.S. Environmental Protection Agency (EPA). The simple, rapid and ultrasensitive Raman detection strategy based on the Ag dendritic nanostructures exhibits great practical potential for the on-site environmental monitoring and the fingerprint identification of trace harmful chemicals in agricultural products and environments.

Acknowledgements

This work was supported by the program of oversea research of Jiangsu DOE .

Notes and references

† Electronic Supplementary Information (ESI) available: [details of any supplementary information available should be included here]. See DOI: 10.1039/b000000x/

1 M. Fleischmann, P. J. Hendra and A. J. Mcquillan, *Chem. Phys. Lett.*, 1974, **26**, 163
2 P. L. Stiles, J. A. Dieringer, N. C. Shah and R. P. Van Duyne, *Annu. Rev. Anal. Chem.* 2008, **1**, 601.
3 a) K. Hering, D. Cialla, K. Ackermann, T. Dorfer, R. Moller, H. Schneidewind, R. Mattheis, W. Fritzsche, P. Rosch and J. Popp, *Anal. Bioanal. Chem.* 2008, **390**, 113; b) M. D. Porter, R. J. Lipert, L. M. Siperko, G. Wang and R. Narayanana; *Chem. Soc. Rev.* 2008, **37**, 1001; c) H.Cui,P.Liu,G.W.Yang, *Applied Physics Letters*,2006,**89** , 153124.
4 H. Ko, S. Singamaneni and V. V. Tsukruk, *Small.* 2008, **4**, 1576.
5 L. D. Qin, S. L. Zou, C. Xue, A. Atkinson, G. C. Schatz and C. A. Mirkin, *Proc. Natl. Acad. Sci. U.S.A.* 2006, **103**, 13300.
6 C. H. Lee, L. M. Tian and S. Singamaneni, *ACS Appl. Mater. Inferfaces* 2010, **2** ,3429.
7 L. M. Chen and Y. N. Liu, *ACS Appl. Mater. Inferfaces* 2011, **3** ,3091.
8 X. Z. Zhou, Y. Zhou, J. C. Ku, C. Zhang and C. A. Mirkin, *ACS Nano* 2014, **8**, 1511.
9 Gutes.A, Carraro.C,Maboudian.R, *J. Am. Chem. Soc,* 2010，**132**, 1476.
10 G. Lu, H. Li and H. Zhang, *Chem. Commun.*, 2011, **47**, 8560.
11 H. Kang, C. J. Heo, H. C. Jeon, S. Y. Lee and S. M. Yang, *ACS Appl. Mater. Inferfaces* 2013, **5**, 4569.
12 H.B.Li,P.Liu,Y.Liang,J.Xiao,G.W.Yang,*Nanoscale.*2012,**4**, 5082.
13 M.J. Siegfried， K.S. Choi，*Angew. Chem. Int. Ed.*, 2008，**47**，368.
14 A. K. Malik and W. Faubel, *Pestic. Sci.* 1999, **55**, 965.
15 V. K. Sharma, J. S. Aulakh and A. K. Malik, *J. Environ. Monit.* 2003, **5**, 717.
16a)Y.Yang,Z.Y.Li,K.Yamaguichi,M.Tanemura,Z.G.Huang,D.L.Jiang,Y. H.Chen,M.Nogami, *Nanoscale*,2012, **4**, 2663. b) Y. Yang, M. Tanemura, Z.G. Huang, D.L. Jiang, Z.Y. Li, Y.P Huang, G. Kawamura, K. Yamaguchi, M. Nogami, *Nanotechnology*, 2010,**21**, 325701.
17 Krieger, A toxicological assessment of sulfur as a pesticide, in *Hayes' Handbook of Pesticide Toxicology*, ed. D. K. Gammon, T. B. Moore and M. A. O'Malley, Academic Press, New York, 2010, vol. **1**, 1889.
18 A. K. Malik and A. L. J. Rao, *Talanta*, 1990, **37**, 1205.
19 C. Fernández, A. J. Reviejo, L. M. Polo, and J. M. Pingarrón, *Talanta*, 1996, **43**, 1341.
20 Y. G. Zhao, X. W. Zheng, Z. Y. Huang, M. M. Yang, *Anal. Chim. Acta*, 2003, **482**, 29.
21 V. K. Sharma, J. S. Aulakh and A. K. Malik, *Talanta*, 2005, **65**, 375.
22 C. Yuan, R. Y. Liu, S. H. Wang, G. M. Han, M. Y. Han, C. L. Jiang and Z. P. Zhang, *J. Mater. Chem*. 2011, **21**, 16264.
23 E. B. Rupp, P. Zuman, I. Šestáková and V. Horák, *J. Agric. Food Chem.* 1992, **40**, 2016.
24 A. Kumar, H. A. Biebuyck and G. M. Whitesides, *Langmuir* 1994, **10**, 1498.

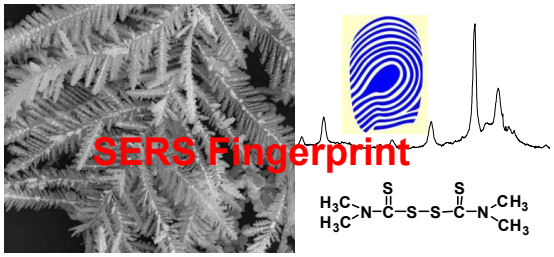

We have developed a SERS-active substrate based on Ag dendritic nanostructures for sensitive Raman signal readout and fingerprint identification of pesticide residues in agricultural products and environments.